Growth of Pure β-Si_3N_4 Nanorods from the Synergic Nitrogen Sources

Fen Xu, Xu Zhang, Wang Xi, Jie Hong, and Yi Xie*
Structure Research Laboratory and Department of Chemistry, University of Science and Technology of China, Hefei, Anhui 230026, P. R. China

(Received January 6, 2003; CL-030013)

Pure β-Si_3N_4 nanorods with of 30–60 nm and length of 180–300 nm were synthesized from a mild benzene-thermal route at 450 °C, starting from $SiCl_4$ and the synergic nitrogen sources of $NaNH_2$ and NH_4Cl. The obtained sample was characterized by XRD, TEM and XPS. The one-dimensional growth mechanism is assumed to be a vapor-liquid-solid (VLS) process.

Silicon nitride (Si_3N_4) is used in a variety of important technological applications. The high fracture toughness, hardness and wear resistance of Si_3N_4-based ceramics are exploited in cutting tools and antifriction bearings.[1] In addition, Si_3N_4 is used as an insulating, masking and passivating materials in electronic applications.[2] Conventional synthetic methods for Si_3N_4 powder often include direct nitridation, carbothermal reduction, a silicon-sulfur-nitrogen reaction between SiS_2 and NH_3, vapor phase reactions, and thermal decomposition.[3–9] These synthetic techniques usually require heating at elevated temperature for long periods of time, high post-treatment temperature (>1200 °C) and high production cost due to their slow growth rate. Self-propagating high-temperature synthesis (SHS) has also been applied successfully to silicon nitridation in nitrogen atmosphere,[10–13] in which an igniting agent (i.e. Ti + C) and the necessary additive (i.e. NH_4F) were used. Recently, Hu et al. employed the reaction of $SiCl_4$ with NaN_3 at about 670 °C under a pressure of about 45 MPa,[14] in which $SiCl_4$ acted as both the reagent and the solvent, but only the mixture of α- and β-phases of Si_3N_4 nanopowder was obtained.

Very recently, a lot of work on the preparation of one-dimensional structures has been done and important progress has been made. Nanotubes and nanowires exhibit a wide range of electronic and optical properties, which depend sensitively on their sizes and shapes.[15–17] However, there is relatively little work on the preparation of β-Si_3N_4 nanorods.

Herein, we described the use of the reaction among $SiCl_4$, $NaNH_2$ and NH_4Cl in benzene at 450 °C in autoclave to prepare β-Si_3N_4 nanorods. In this work, we successfully employed the synergic nitrogen sources of $NaNH_2$ and NH_4Cl and obtained the pure β-Si_3N_4 nanorods.

In a typical process, 36 mL $SiCl_4$, 0.96 g $NaNH_2$ and 0.32 g NH_4Cl were placed in a titanium alloy autoclave of about 50 mL capacity, and then 9 mL benzene was added till up to 90% volume. Excess $SiCl_4$ was used to adjust the pressure in the process and the reaction temperature, thereby guaranteed the thorough completion of the reaction. After deaerated with bubbling with nitrogen gas for 30 min, the autoclave was steeled and maintained at 450 °C for 6 h, then cooled to room temperature on standing. The product was filtered out and washed with benzene to remove the unreacted $SiCl_4$ followed by dilute HF and distilled water to remove NaCl and other impurities. Finally, the gray-white product was dried in vacuum at 60 °C for 3 h.

The XRD[18] pattern corresponding to powders with random orientation is shown in Figure 1. The peaks in Figure 1 can be indexed as β-Si_3N_4 with a hexagonal cell with lattice parameters: $a = 7.693$ Å, $c = 2.926$ Å, which are consistent with the literature values (JCPDS cards No. 33-1160: $a = 7.6044$ Å, $c = 2.9075$ Å). The intensity of (111) peak increases while those of (110), (210), (101) peaks decrease, indicating the anisotropic growth of the β-Si_3N_4 crystals.

Figure 2 shows the TEM[18] micrograph of the sample as well as the corresponding selected area electron diffraction pattern. The TEM image reveals β-Si_3N_4 nanorods with diameters of 30–60 nm and length of 180–300 nm (Figure 2a), and the SAED pattern clearly shows the single crystalline nature of the β-Si_3N_4 nanorods and that the nanorod axis is close to the [001] direction (Figure 2b). From this and the XRD data, it can be concluded that the nanorod axis is indeed [001].

The XPS[18] spectra (Figure 3) show the composition of β-Si_3N_4 nanorods. The binding energy of N_{1s} and Si_{2p} are 397.6 eV and 101.7 eV, as shown in Figures 3a and 3b, respectively, and the quantification of peaks gives a Si:N ratio of 3.2:4. No other impurities peaks were observed.

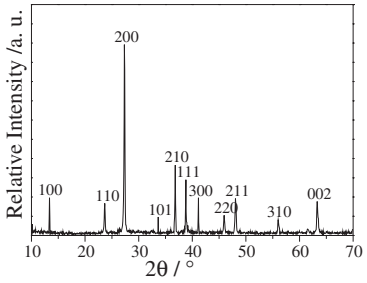

Figure 1. XRD pattern of the as-prepared β-Si_3N_4 nanocrystals.

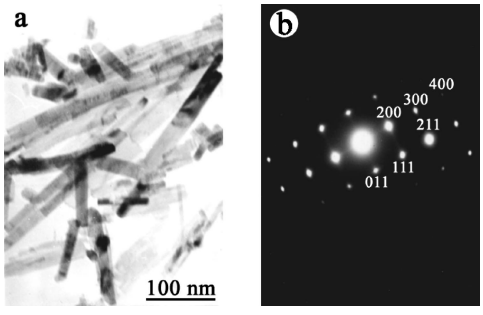

Figure 2. (a) TEM image of β-Si_3N_4 nanorods and (b) the corresponding selected-area electron pattern (SAED).

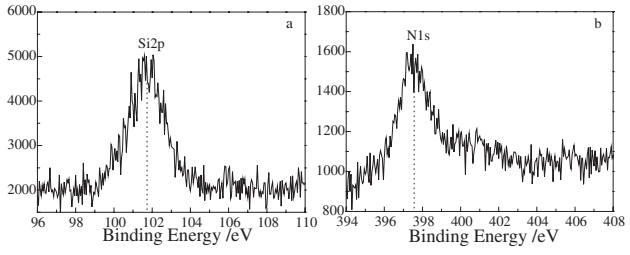

Figure 3. XPS spectra of β-Si_3N_4 nanorods (a) Si 2p region and (b) N 1s region.

Our approach to β-Si_3N_4 nanorods is essentially based on the solvothermal reaction among $SiCl_4$, Na_3N and NH_3. It is well-known that $NaNH_2$ would decompose to Na_3N by loss of ammonia on heating[19] and NH_4Cl can also decompose to NH_3 on heating, as described in the following Eqs. 2 and 1. The renascent Na_3N and NH_3 can be regarded as the intermediate reactants and immediately reacted with $SiCl_4$ to form β-Si_3N_4 nanocrystals, as represented in the Eq. 3. According to free energy calculation, the reaction between $SiCl_4$ and the synergic nitrogen source of $NaNH_2$ and NH_4Cl, described as the total equation, is thermodynamically driven to the right side and highly exothermic ($\Delta G_f^o = -696.36\,kcal\cdot mol^{-1}$, $\Delta H_f^o = -358.84\,kcal\cdot mol^{-1}$).[20] In the comparison experiments, only amorphous Si_3N_4 was obtained at 450 °C, even at 500 °C, if either single nitrogen source $NaNH_2$ or NH_4Cl was used. It is the synergic effect resulting from the nitrogen sources that makes β-Si_3N_4 to crystallize at rather lower temperature. The reactions involved here are as follows:

$$NH_4Cl \longrightarrow NH_3+HCl \quad (1)$$

$$3NaNH_2 \longrightarrow Na_3N+2NH_3 \quad (2)$$

$$3SiCl_4+Na_3N+3NH_3 \longrightarrow \beta\text{-}Si_3N_4+3NaCl+9HCl \quad (3)$$

$$3SiCl_4(l)+3NaNH_2+NH_4Cl \xrightarrow{723\,K} \beta\text{-}Si_3N_4+3NaCl+10HCl(g)$$

Among the three well-known whisker-growth mechanisms, namely, solution-liquid-solid (SLS), vapor-solid (VS), and vapor-liquid-solid (VLS), the VLS mechanism is most likely to function under the present condition because this case involves the reaction in organic solvent, and uses $SiCl_4$ liquid reactant and the intermediate reactants including NH_3 gas reactant. In this system, $SiCl_4$ is much excess and is soluble in benzene. The surface of the $SiCl_4$–benzene mixture may have a large accommodation coefficient and is, therefore, a preferred site for the deposition of atoms from the vapor phase reactant NH_3, which can benefit the VLS nucleation for the β-Si_3N_4 nanorods. A feature of this synthesis route is the high pressure in the autoclave, coming from NH_3 and benzene, which may facilitate the VLS nucleation of the β-Si_3N_4 nanorods.

In summary, samples of 30–60 nm × 180–300 nm β-Si_3N_4 nanorods were successfully synthesized via the reaction of $SiCl_4$ with the synergic nitrogen sources of $NaNH_2$ and NH_4Cl at 450 °C under benzene-thermal conditions. The synergic nitrogen sources play a crucial role in the formation of β-Si_3N_4 nanocrystallites. The VLS mechanism is likely to be responsible for the one-dimensional growth.

Financial supports from the National Natural Science Foundation of China and Chinese Ministry of Education are gratefully acknowledged.

References and Notes

1 K. Komeya and M. Matsui, in "Materials Science and Technology," ed. by R. W. Cahn, P. Haasen and E. J. Kramer, Weinheim, Wiley-VCH (1994).
2 "Gmelin Handbook of Inorganic and Organometallic Chemistry," Si Suppl. B. 5c, Silicon Nitride in Electronic, Berlin, Springer (1991).
3 M. Ekelund and B. Forslund, *J. Am. Ceram. Soc.*, **75**, 532 (1992).
4 T. Licko, V. Figusch, and Púchyová, *J. Eur. Ceram. Soc.*, **9**, 219 (1992).
5 J. Janiga, K. P. Sin, and V. Figusch, *J. Eur. Ceram. Soc.*, **8**, 153 (1991).
6 T. Yamada, *Am. Ceram. Soc. Bull.*, **72**, 99 (1993).
7 K. S. Mazdiyasni and C. M. Cooke, *J. Am. Ceram. Soc.*, **56**, 628 (1973).
8 P. E. D. Morgan, *Mater. Res. Soc. Symp. Proc.*, **32**, 213 (1984).
9 W. R. Cannon, S. C. Danforth, J. H. Flint, J. S. Haggerty, and R. A. Marra, *J. Am. Ceram. Soc.*, **65**, 324 (1982).
10 A. G. Merzhanov and I. P. Borovinskaya, *Combust. Sci. Technol.*, **10**, 195 (1975).
11 W.-C. Lee and S.-L. Chung, *J. Mater. Res.*, **12**, 805 (1997).
12 M. A. Rodriguez, N. S. Makhonin, J. A. Escriña, I. P. Borovinskaya, M. I. Osendi, M. F. Barba, J. E. Iglesias, and J. S. Moya, *Adv. Mater.*, **7**, 745 (1995).
13 D. Y. Chen, B. L. Zhang, H. R. Zhuang, W. L. Li, and S. Y. Xu, *Mater. Res. Bull.*, **37**, 1481 (2002).
14 K. B. Tang, J. Q. Hu, Q. Y. Lu, Y. Xie, J. S. Zhu, and Y. T. Qian, *Adv. Mater.*, **11**, 653 (1999).
15 P. Yan, Y. Xie, Y. T. Qian, and X. M. Liu, *Chem. Commun.*, **1999**, 1293.
16 X. F. Duan and C. M. Lieber, *J. Am. Chem. Soc.*, **122**, 188 (2000).
17 T. J. Trentler, K. M. Hickman, S. C. Goel, A. M. Viano, P. C. Gibbons, and W. E. Buhro, *Science*, **270**, 1791 (1995).
18 XRD measurement was carried out on a Japan Rigaku D/max rA X-ray diffractometer equipped with graphite monochromatized high-intensity Cu-Kα radiation ($\lambda = 1.54178$ Å). The TEM image and ED pattern were taken on a Hitachi Model H-800 instrument with a tungsten filament, using an accelerating voltage of 200 kV. XPS spectra were recorded on a VGESCALAB MKII X-ray photoelectron spectrometer. XPS data were collected in the constant analyzer energy (CAE) made at 20 eV with Mg Kα ($h\nu = 1253.6$ eV) radiation as the excitation source.
19 F. A. Cotton, G. Wilkinson, C. A. Murillo, and M. Bochmann, "Advanced Inorganic Chemistry," John Wiley and Sons, Inc. (1999).
20 J. A. Dean, "Lange's Handbook of Chemistry," 13th ed., McGraw-Hill, New York (1985).

Published on the web (Advance View) June 17, 2003; DOI 10.1246/cl.2003.600